

Efficient Synthesis of NIR Emitting Bis[2-(2'-hydroxyphenyl)benzoxazole]
Derivative and Its Potential for Imaging Applications

Junfeng Wang, Hannah Baumann, Xiaoman Bi, Leah P. Shriver, Zhaoda
Zhang, Yi Pang

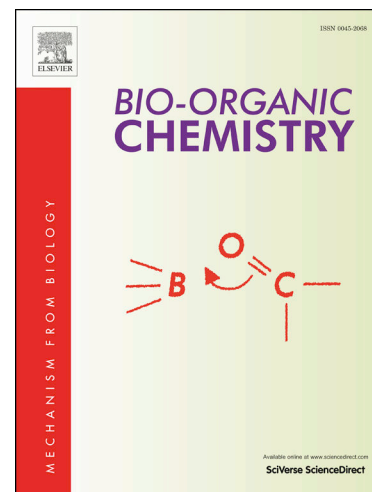
PII: S0045-2068(19)31265-9
DOI: <https://doi.org/10.1016/j.bioorg.2020.103585>
Reference: YBIOO 103585

To appear in: *Bioorganic Chemistry*

Received Date: 2 August 2019
Revised Date: 12 January 2020
Accepted Date: 13 January 2020

Please cite this article as: J. Wang, H. Baumann, X. Bi, L.P. Shriver, Z. Zhang, Y. Pang, Efficient Synthesis of NIR Emitting Bis[2-(2'-hydroxyphenyl)benzoxazole] Derivative and Its Potential for Imaging Applications, *Bioorganic Chemistry* (2020), doi: <https://doi.org/10.1016/j.bioorg.2020.103585>

This is a PDF file of an article that has undergone enhancements after acceptance, such as the addition of a cover page and metadata, and formatting for readability, but it is not yet the definitive version of record. This version will undergo additional copyediting, typesetting and review before it is published in its final form, but we are providing this version to give early visibility of the article. Please note that, during the production process, errors may be discovered which could affect the content, and all legal disclaimers that apply to the journal pertain.



Efficient Synthesis of NIR Emitting Bis[2-(2'-hydroxyphenyl)benzoxazole] Derivative and Its Potential for Imaging Applications

Junfeng Wang,^{a,c,d} Hannah Baumann,^a Xiaoman Bi,^a Leah P. Shriver,^a Zhaoda Zhang,^d and Yi Pang^{*ab}

^a Department of Chemistry & ^bMaurice Morton Institute of Polymer Science, The University of Akron, Akron, OH, USA, 44325

^c Gordon Center for Medical Imaging, Massachusetts General Hospital and Harvard Medical School, 125 Nashua Street, Boston, MA, 02114

^d Martinos Center for Biomedical Imaging, Massachusetts General Hospital and Harvard Medical School, 149, 13th st, Charlestown, MA, 02129

* Email: yp5@uakron.edu

Abstract: Unassymetric bis[2-(2'-hydroxyphenyl)benzoxole]] bis(HBO) derivatives with a DPA functionality for zinc binding have been developed with an efficient synthetic route, using the retrosynthetic analysis. Comparison of bis(HBO) derivatives with different substitution patterns allows us to verify and optimize their unique fluorescence properties. Upon binding zinc cation, bis(HBO) derivatives give a large fluorescence turn-on in both visible ($\lambda_{em} \approx 536$ nm) and near-infrared (NIR) window ($\lambda_{em} \approx 746$ nm). The probes are readily excitable by a 488 nm laser, making this series of compounds a suitable imaging tool for *in vitro* and *in vivo* study on a confocal microscope. The application of zinc binding-induced fluorescence turn-on is successful demonstrated in cellular environments and thrombus imaging.

Keywords: Fluorescent probe; Near Infrared; Benzoxazole; ESIPT; Zinc; Thrombus imaging

Introduction

In recent years, fluorescent sensors are emerging as powerful tools for molecular imaging.¹ In this attractive field, there are increasing interests to develop optical probes that give emission in the near-infrared (NIR) region (650-900 nm). This is because the NIR photons can penetrate deeply through biological tissues, thereby enabling detection of molecular activity for *in vivo* applications.²⁻⁷ An ideal NIR probe should also exhibit a large Stokes' shift, in order to have minimum interference between excitation and emission signals. Additionally, a qualified NIR probe should be integrated with a suitable chemical event that can generate a large optical response when responding to a specific analyte of interest.⁸

2-(2'-Hydroxyphenyl)benzoxazole (HBO) derivatives represent an interesting class of dyes, which exhibit a large Stokes' shift (> 150 nm) arising from the excited-state intramolecular proton transfer (ESIPT).^{9,10} The photochemical event is dependent on the presence of the phenolic proton, whose migration to the "nitrogen" allows the formation of its corresponding *keto* tautomer with emission at a longer wavelength. The metal chelation to mono HBO system, however, removes the phenolic proton, thereby eliminating the ESIPT.^{11,12} In an effort to overcome the barrier and enable the ESIPT from a metal-HBO complex, we recently show that 2, 5-bis(benzoxazole-2-yl)benzene-1,4-diol derivatives **1**, bis(HBO), can exhibit a remarkable optical response upon zinc binding, giving the turn-on emission in both visible (at ~ 550 nm) and NIR regions (at ~ 750 nm).¹³⁻¹⁵ The chemical event for the sensor response is dependent on the formation of **2**, where the zinc complexation acts as an effective switch to turn-on the ESIPT emission (corresponding to the

emission in NIR region). In the molecular design of **1**, a 2, 2'-dipicolylamine (DPA) group is attached to selectively bind Zn^{2+} cation, while a remaining HBO is used to enable the ESIPT. The choice of DPA ligand is based on its high selectivity to Zn^{2+} cation. Despite the impressive sensor performance of **1b** (low toxicity and large response to Zn^{2+} binding),¹⁵ the synthesis of **1** suffers from low yields, which hamper its broad application. The previous synthesis was based on a linear *consecutive* sequence consisting of 8 steps,^{15,16} which makes it difficult to access this class of compounds for extensive studies. In an continuing effort to overcome the barrier, we now report a highly efficient synthesis of 2, 5-bis(HBO) derivatives with a DPA functionality, by adopting a *convergent* synthetic strategy. In the synthesis design, the target molecule was disconnected in the middle to give two fragments **A** and **B** (Scheme 1), thereby leading to improved yields.

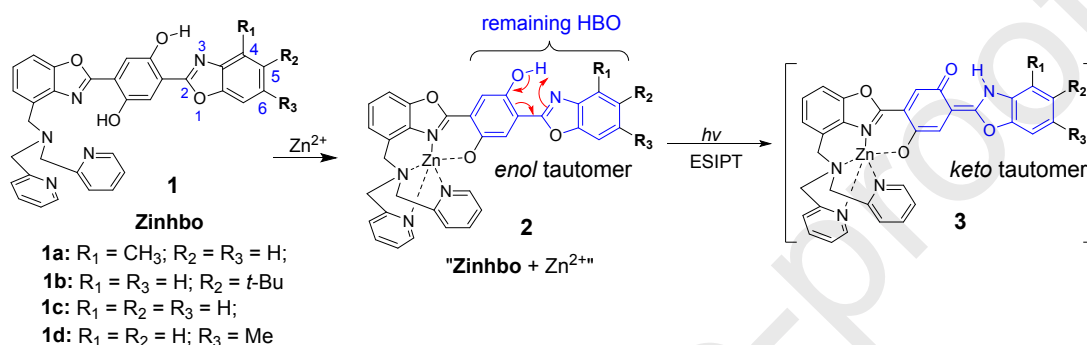
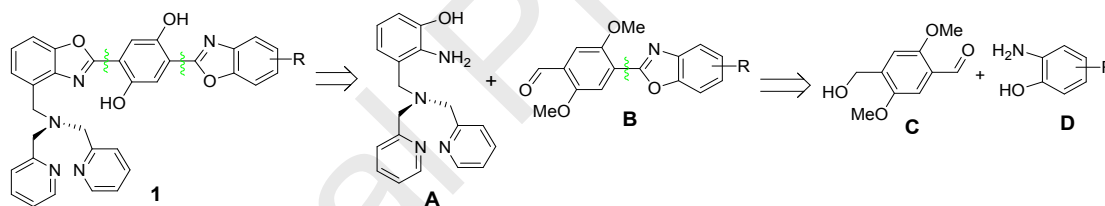


Figure 1. Chemical structure of Zinhbo compounds **1** as well as the *enol* and *keto* tautomer structures of the corresponding zinc complex.



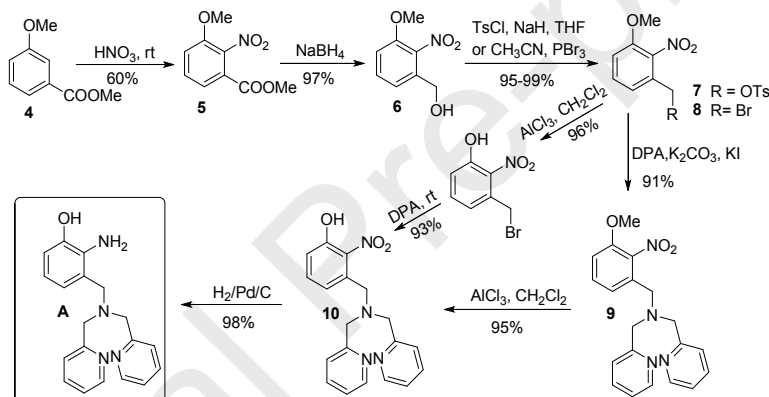
Scheme 1. Retrosynthetic analysis of the bis(HBO) derivatives.

In the previous synthesis of **1b**,¹⁵ the low yield was associated with the introduction of the DPA group, which was accomplished by using a sequence of low-yielding reactions to accomplish the transformation $\text{Ar-CH}_3 \rightarrow \text{Ar-CH}_2\text{-N}(\text{CH}_2\text{-py})_2$. Although an improved methodology was developed to synthesize Zinhbo compounds with higher yields, the reduction of the carboxylic ester group in the synthesis greatly limited the diversity of these derivatives.¹⁶ Herein we report a new strategy for efficient synthesis of bis(HBO) derivatives, which is based on a retrosynthetic analysis involving the bond disconnections in the middle of the target to give two fragments **A** and **B** (Scheme 1). The synthetic direction can be outlined as follows: (1) preparation of the key intermediate **A**, which incorporates the DPA group in the early stage; (2) efficient synthesis of benzoxazole **B** from aldehyde **C** and 2-amino-phenol **D**; (3) reaction of **A** and **B** to give the bis(HBO) products.

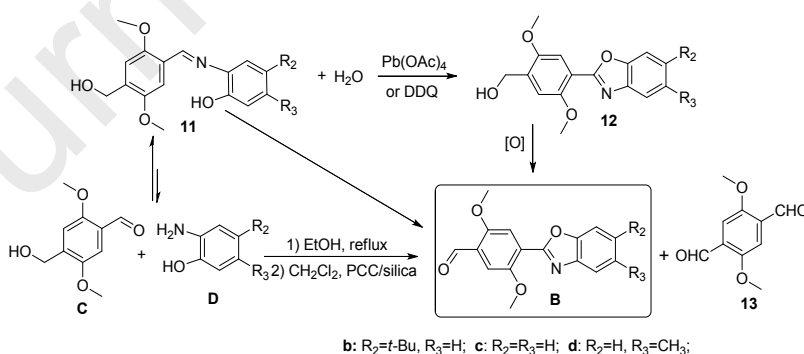
Results and Discussion

Scheme 2 presents the construction of the key intermediate **A**. Thus compound **5** was prepared conveniently by the nitration of **4** with nitric acid at room temperature, which precipitated from

the solution and was recrystallized from EtOAc/hexane as large colorless crystals (50-60% yield). Selective reduction of ester **5** by NaBH₄ in THF/MeOH^{17,18} proceeded cleanly to furnish alcohol **6**, which then underwent tosylation or bromination to provide corresponding **7** or **8** in almost quantitative yields.^{19,20} Reaction of **7** or **8** with 2, 2'-dipicolylamine (DPA) in the presence of K₂CO₃ and KI gave compound **9** in good yields.²¹ Deprotection of the methoxy group proceeded smoothly at room temperature by using AlCl₃ to give **10**,²² which was then reduced by H₂ over Pd/C to afford the intermediate **A** in almost quantitative yield. Although the procedure was quite satisfactory on a small scale (e.g., 1 mmol), the deprotection of **9** by AlCl₃ was found to be troublesome for a larger scale reaction (e.g., 5 mmol). The reaction was not completed even by using a large excess of AlCl₃. This is because some syrup-like residues precipitated out during the reaction, possibly due to (a) chelation of AlCl₃ with DPA, and (b) encapsulation of unreacted **9**. In order to overcome the deficiency in the deprotection of **9**, our attention was directed to seek deprotection of the methyl phenol ether at an earlier stage, i.e. before introduction of DPA. Attempts to deprotect the methyl from the phenol ether **6** gave low yield by using either AlCl₃ or BBr₃. However, the methyl group of **8** was removed effectively by using AlCl₃ to give 3-(bromomethyl)-2-nitrophenol, which could be converted to **10** in high yield.



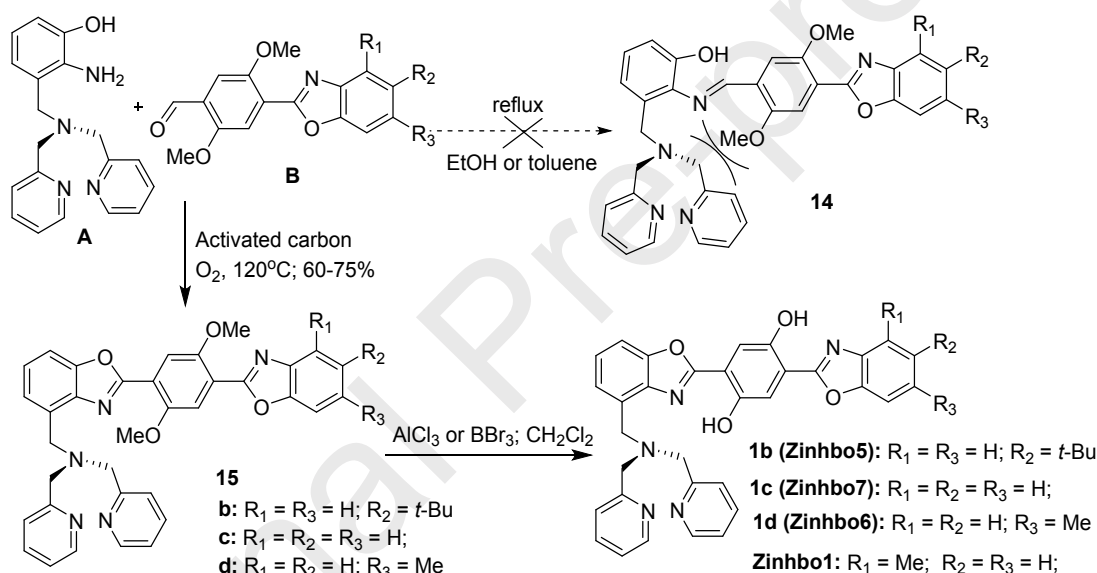
Scheme 2. Synthesis of key intermediate **A**.



Scheme 3. Synthesis of key intermediate **B**.

The construction of the benzoxazole fragment **B** from intermediate **C** and 2-aminophenols **D** (Scheme 3) was also significantly improved with a one-pot reaction. In the synthesis of benzoxazole compounds, most reported methods require the isolation of the imine intermediate **11**, followed by an oxidative cyclization to form the benzoxazole intermediate **12**.²³⁻²⁹ Although DDQ and Pb(OAc)₄ worked well for oxidative cyclization of **11**,¹³⁻¹⁵ the reaction typically gave

the alcohol **12** without further oxidation. An additional oxidation step was thus required to further oxidize the alcohol **12** with another oxidant, in order to obtain the aldehyde **B**. In other words, the reaction sequence **11**→**12**→**B** could be accomplished by involving two steps of oxidation. An intriguing question is whether one can find a suitable oxidant that can execute both “oxidative cyclization” and “oxidation of the alcohol to the aldehyde”, thereby greatly simplifying the reaction procedure. Bearing this in mind, we decided to examine PCC which is known to oxidize primary alcohols to aldehydes and to oxidize imine to benzoxazoles as well.³⁰ Simple mixing of **C** and **D** with PCC in CH₂Cl₂ led to **B** in 26% yield, and a large amount of byproduct was identified as **13**. The initial result indicated that PCC was effective for both cyclization and oxidation. Interestingly, when using TLC to monitor the reaction, we found **C** and **D** reacted quickly on TLC plate, forming imine intermediate **11**. This observation encouraged us to optimize the reaction conditions with silica gel and PCC. After extensive trials, a *one-pot* multistep method for the synthesis of **B** (by direct reaction between **C** and **D**) was developed in 60-80% yield with high reproducibility by silica gel and PCC.



Scheme 4. Construction of bis(HBO) system (Zinhbo dyes).

Finally, the coupling of **A** and **B** was studied (Scheme 4). Unfortunately, all the reported catalysts and reagents such as Mn(OAc)₃,²⁶ KAl(SO₄)₂,²⁷ Pb(OAc)₄,²⁸ Ba(MnO₄)₂,²⁹ DDQ and even the PCC/silica gel method failed to give any desirable **15** (Scheme 4). It was found that the imine **14** was not formed by refluxing **A** and **B** in EtOH or toluene overnight, probably due to the steric hindrance. After exhaustive exploration, fortunately, we found that Tagawa's method using O₂ with activated carbon gave **15** in up to 72% yield.³¹ The final product **1b** could be easily prepared by the deprotection of methoxy groups catalyzed by AlCl₃ or BBr₃ in anhydrous CH₂Cl₂. With the availability of the intermediate **A**, the products (**1b-1d**) could be effectively synthesized in 2 steps in high yields.

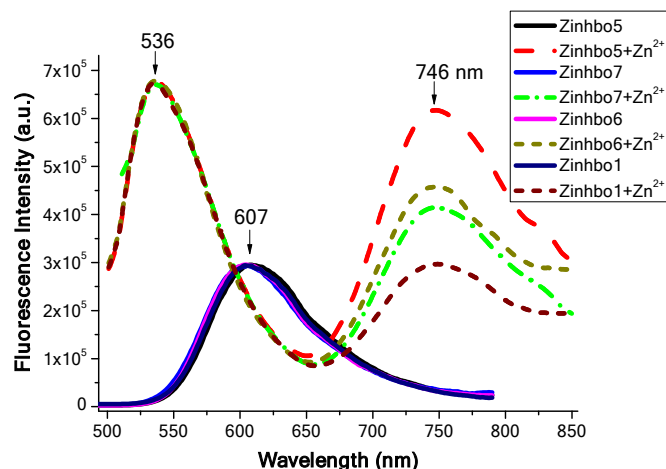
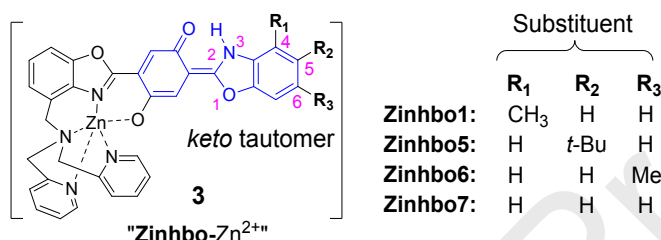


Figure 2 Normalized fluorescence spectra of **Zinhbo** compounds (5 μ M; excitation at 414 nm) and **Zinhbo-Zn²⁺** complexes (formed upon addition of 1 equiv Zn²⁺) in CH₂Cl₂ (excitation at 480 nm). The spectra are normalized at 607 nm for **Zinhbo**, and at 536 nm for **Zinhbo-Zn²⁺** complexes.



Scheme 5. Chemical structures of *keto* tautomer of Zinhbo-Zn complexes.

Fluorescent properties and imaging application. The newly developed synthetic strategy allowed us to obtain Zinhbo-6 and Zinhbo-7, in addition to the previously reported Zinhbo-1¹³ and Zinhbo-5.¹⁵ Optical properties of these Zinhbo compounds (Scheme 5) allowed us to examine the possible substituent effect. Fluorescence spectra of these Zinhbo compounds revealed one emission peak ($\lambda_{em} \approx 607$ nm) (Figure 2). Upon binding Zn²⁺, the resulting Zinhbo-Zn²⁺ complexes gave two characteristic emission peaks ($\lambda_{em} \approx 536, 746$ nm), corresponding to their *enol* and *keto* tautomers (**2** and **3**, respectively). The ability of using Zn²⁺ binding to generate two well separated emission is a unique property of Zinhbo compounds. In the study, one fundamental question is how the structure can be modified to affect the NIR emission wavelength and its intensity. In order to make comparison, the fluorescence spectra were normalized at the green emission peak ($\lambda_{em} \approx 536$, Figure 2). The alkyl substituent on 4-, 5-, and 6-position exhibited essentially no effect on the emission wavelength. However, the positions of alkyl substituents significantly influenced the relative NIR emission intensity, which could be attributed to the electronic perturbation by the substituents. The position of the alkyl substituents was found to affect not only the NIR emission, but also the quantum yield (ESI, Table S1). However, Zinhbo-5 remained to be the best among them in terms of the strong NIR emission (Figure 2 and ESI, Figure S2).

The ability of Zinhbo-5 to give simultaneous emission in both green and NIR channels, when responding to Zn²⁺ binding,¹⁵ encouraged us to use the probe on confocal microscope study, which has not been examined before. Since the probe-Zn²⁺ complex can be excited readily by a 488 nm laser, it would be a useful tool for imaging exogenous and endogenous Zn²⁺ ions in living cells

(Figure 3). Thus, Hela cells were stained with Zinhbo-5 (10 μM) in culture medium with prolonged incubation time (60 min) at 37°C, we were delighted to find observable green and NIR signal, which reveals the great sensitivity of this sensor. With exogenous Zn^{2+} ions (10 μM), very strong green and NIR signals were obtained on the confocal image throughout the cytoplasm. This further proved the great sensitivity and bio-compatibility of the sensor. As far as we know, this is the first successful *in vitro* zinc selective NIR turn-on imaging with ESIPT property (> 270 nm stokes' shift).

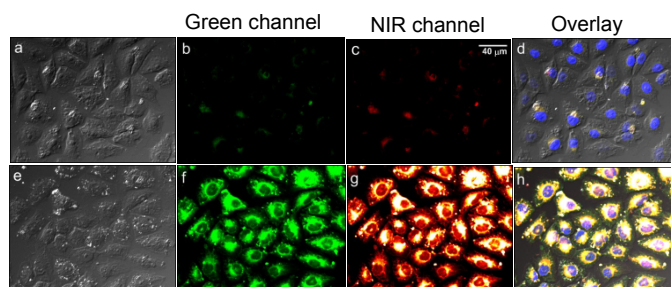


Figure 3. Top: Fluorescence images of Hela cells incubated with 10 μM Zinhbo-5 for 60 min at 37°C in cell culture medium; Bottom: Hela cells were first treated with 10 μM Zn^{2+} for 30 mins, washed 3 times with PBS, the cells were further incubated with 10 μM Zinhbo-5 for another 60 min at 37°C in cell culture medium. The experiments were carried out on an Olympus FV1000 Confocal Microscopy, excited with a 488 nm laser, and the images were collected in both green channel (535-565 nm) and NIR channel (700-750 nm).

In order to examine the probe's general utility, Zinhbo-5 was further used to stain oligodendrocytes that are myelinating glial cells of the central nervous system. Thus, to the MO3.13 cells media (oligodendrocytes) were treated with TPEN (*N,N,N',N'*-tetrakis(2-pyridylmethyl)ethylenediamine) that is a high-affinity zinc chelator, washed with cell medium and added Zinhbo-5 (5 μM). The fluorescence confocal imaging revealed that Zinhbo-5 readily stained the cells (Figure 4). While the fluorescence signal of Zinhbo-5 was very weak in the absence of Zn^{2+} (Figure 4d), addition of Zn^{2+} induced a large fluorescence turn-on (Figure 4e and 4f). Similar results were also obtained when staining Fibroblast cells. These results illustrated that Zinhbo-5 could be a useful probe for monitoring cellular zinc level.

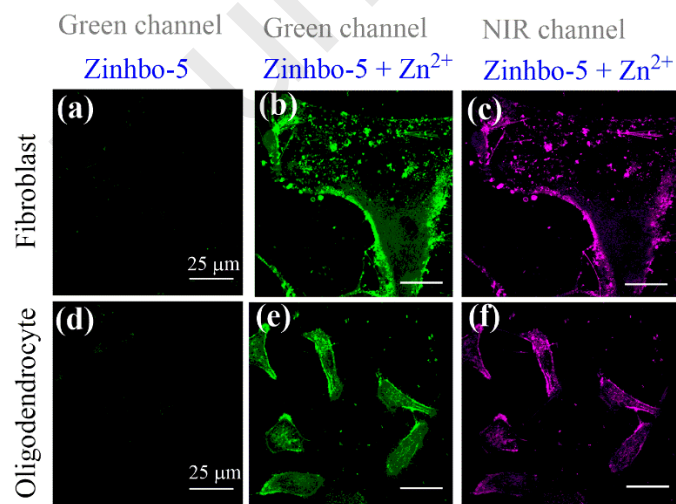


Figure 4. Confocal imaging of fibroblast (top row) and oligodendrocyte cells (bottom row) treated with TPEN (50 μ M), washed with cell medium, and incubated with Zinhbo-5 (5 μ M) for 30 min (images a & d; Ex/Em= 488/525 nm), followed by treatment with 50 μ M Zn^{2+} for 30 mins in green channel (b and e, Ex/Em= 488/525 nm) and NIR channel (c and f; Ex/Em= 488/700 nm).

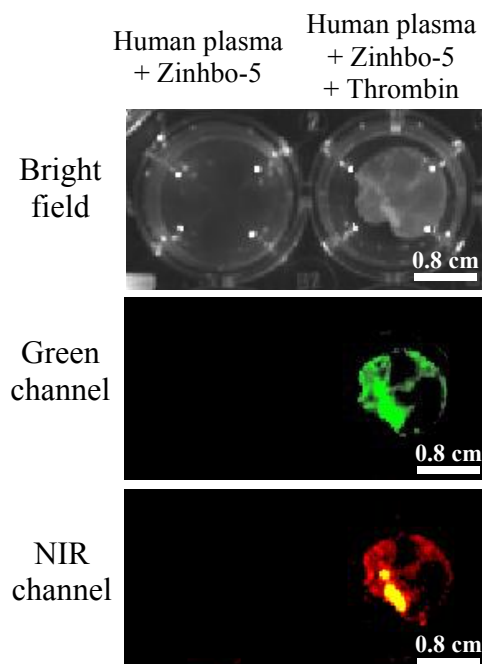


Figure 5. *In vitro* NIR imaging of thrombus by using Zinhbo-5. Top row: Human plasma (0.5 mL) containing 1.0 μ M of Zinhbo-5 (left well); Human plasma containing 1.0 μ M of Zinhbo-5, followed by addition of 1.0 μ L of 1Unit/mL thrombin (right well, from Millipore Sigma, Cat. No. 605160). Middle and bottom rows: Human plasma and resulting clots were imaged with Ex/Em = 465/560 nm (Green channel) or Ex/Em = 465/760 nm (NIR channel) using an IVIS[®] Spectrum imaging system.

Cell viability of **Zinhbo-5** was checked with HEK293 cells in DMEM medium, by using alamar blue assay. No significant cell toxicity was observed up to 48 hours of the cells with up to 100 μ M concentration, when the DMSO stock solution (10 mM) was diluted to cell culture medium (ESI Figure S5). The ability of Zinhbo-5 in responding to cellular Zn^{2+} , in addition to its low toxicity, encouraged us to seek its further application. An interesting problem is blood clot, which is formed when responding to the blood vessel injury (e.g. resulting from cuts and bruises) in order to prevent bleeding. However, blood clot in the absence of injury (called thrombus) can be dangerous, as it can block a key blood vessel to impede blood flow, leading to cardiovascular diseases such as heart attack, stroke, pulmonary embolism, and deep vein thrombosis. It is known that zinc is involved in thrombosis and thrombolysis, where Zn^{2+} concentration is delicately controlled in the blood.³² When Zn^{2+} cations circulate in plasma at a concentration of 10–20 μ M, most cations are bound to plasma proteins such as albumin (forming a labile, exchangeable pool), but some (about 0.1–2 μ M) are in a free unbound state. Because the platelets in thrombi, which respond to blood vessel damage, are 50-100 folds higher than those found in the circulating blood. Upon activation, Zn^{2+} stored in platelets are released, thereby increasing the free zinc concentrations.³²⁻³⁷ Therefore,

the high Zn^{2+} concentrations in thrombus may enable the zinc sensors for thrombus imaging. To test this hypothesis, the *in vitro* blood clot model was generated by addition of thrombin into the human plasma according to a reported protocol.³⁸ The clear blood clots could be seen within 10-15 min (Figure 5, right well of top row). The significant fluorescence turn-on signals within the clots were displayed in both green and NIR channel (Figure 5, right well). There was no fluorescence signal generated by Zinhbo-5 in the plasma (Figure 5, left well). This result demonstrates that the NIR fluorescence zinc turn-on dyes such as Zinhbo-5 are promising probes for thrombus imaging. To our best knowledge, this is the first thrombus imaging evidenced by an NIR zinc sensor.

In summary, an efficient synthetic route has been developed for the synthesis of bis(HBO) compounds with the zinc-chelating DPA functionality. When using together with silica gel, PCC is found to be effective for accomplishing both “oxidative cyclization” and “oxidation of alcohol” steps, thereby greatly simplifying the reaction sequence. The finding opens a path to access this class of compounds for imaging applications, which are known to exhibit low toxicity and attractive fluorescence¹⁵ but are rather difficult to synthesize. The availability of the bis(HBO) sensor **1** allows us to further examine its potential imaging applications for zinc detection, since it exhibits attractive photophysical properties including large fluorescence turn-on in the desirable NIR region upon zinc binding. The successful *in vitro* NIR imaging for the detection of exogenous and endogenous Zn^{2+} ions in living cells makes this sensor a promising tool for imaging applications. This is further demonstrated by observing significant fluorescence turn-on signals within the blood clots. Study by using the improved synthesis to access other new NIR-emitting zinc sensors is in progress, and their potential applications for imaging zinc-related disease/diagnosis will be reported in another forthcoming manuscript.

Acknowledgements. YP acknowledge support from Coleman endowment (from the University of Akron) and National Institute of Health (Grant No: 1R15GM126438-01A1) and ZZ acknowledge support from NIH National Cancer Institute (NCI) (Grant No: 1R01CA197401).

Appendix A. Supplementary data associated with this article can be found in the online version at <https://doi.org/xxxxxx>.

References

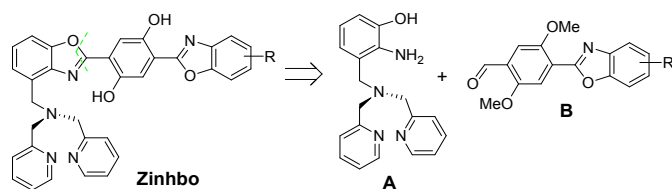
1. Goncalves, M. S. Fluorescent Labeling of Biomolecules with Organic Probes. *Chem. Rev.* **2009**, *109*, 190-212.
2. Guo, Z.; Park, S.; Yoon, J.; Shin, I. Recent progress in the development of near-infrared fluorescent probes for bioimaging applications. *Chem. Soc. Rev.* **2014**, *43*, 16-29.
3. Bremer, C.; Tung, C. H.; Bogdanov, A.; Weissleder, R. Imaging of Differential Protease Expression in Breast Cancers for Detection of Aggressive Tumor Phenotypes. *Radiology* **2002**, *222*, 814-818.
4. Kiyose, K.; Kojima, H.; Nagano, T. Functional Near-Infrared Fluorescent Probes. *Chem. Asian J.* **2008**, *3* (3), 506-515.

5. Licha, K.; Olbrich, C. Optical imaging in drug discovery and diagnostic applications. *Adv. Drug Delivery Rev.* **2005**, *57* (8), 1087-1108.
6. Ntziachristos, V.; Bremer, C.; Weissleder, R. Fluorescence imaging with near-infrared light: new technological advances that enable in vivo molecular imaging. *Eur. Radiology* **2003**, *13*, 195-208.
7. Oushiki, D.; Kojima, H.; Terai, T.; Arita, M.; Hanaoka, K.; Urano, Y.; Nagano, T. Development and Application of a Near-Infrared Fluorescence Probe for Oxidative Stress Based on Differential Reactivity of Linked Cyanine Dyes. *J. Am. Chem. Soc.* **2010**, *132*, 2795-2801.
8. Luo, S. L.; Zhang, E. L.; Su, Y. P.; Cheng, T. M.; Shi, C. M. A review of NIR dyes in cancer targeting and imaging. *Biomaterials* **2011**, *32*, 7127-7138.
9. Formosinho, S. J.; Arnaut, L. G. Excited-state proton transfer reactions II. Intramolecular reactions. *J. Photochem. Photobiol. A : Chem.* **1993**, *75*, 21-48.
10. Sedgwick, A. C.; Wu, L.; Han, H. H.; Bull, S. D.; He, X. P.; James, T. D.; Sessler, J. L.; Tang, B. Z.; Tian, H.; Yoon, J. Excited-state intramolecular proton-transfer (ESIPT) based fluorescence sensors and imaging agents. *Chem. Soc. Rev.* **2018**, *47* (23), 8842-8880.
11. Taki, M.; Wolford, J. L.; O'Halloran, T. V. Emission Ratiometric Imaging of Intracellular Zinc: Design of a Benzoxazole Fluorescent Sensor and Its Application in Two-Photon Microscopy. *J. Am. Chem. Soc.* **2004**, *126* (3), 712-713.
12. Chu, Q.; Medvetz, D. A.; Panzner, M. J.; Pang, Y. A fluorescent bis(benzoxazole) ligand: Toward binuclear Zn(II)-Zn(II) assembly. *Dalton Trans.* **2010**, *39*, 5254-5259.
13. Xu, Y.; Pang, Y. Zinc binding-induced near-IR emission from excited-state intramolecular proton transfer of a bis(benzoxazole) derivative. *Chem. Commun.* **2010**, *46*, 4070-4072.
14. Xu, Y.; Pang, Y. Zn²⁺-triggered excited-state intramolecular proton transfer: a sensitive probe with near-infrared emission from bis(benzoxazole) derivative. *Dalton Transactions* **2011**, *40*, 1503-1509.
15. Xu, Y.; Liu, Q.; Dou, B.; Wright, B.; Wang, J.; Pang, Y. Zn²⁺ Binding-Enabled Excited State Intramolecular Proton Transfer: A Step toward New Near-Infrared Fluorescent Probes for Imaging Applications. *Adv. Healthcare Mater.* **2012**, *1*, 485-492.
16. Wang, J.; Pang, Y. A versatile synthesis of bis[2-(2'-hydroxyphenyl)benzoxazole] derivatives as zinc sensors. *RSC Advance* **2013**, *3*, 10208-10212.
17. Costa, J. C. S. D.; Pais, K. C.; Fernandes, E. L.; Oliveira, P. S. M. D.; Mendonca, J. S.; Souza, M. V. N. D.; Peralta, M. A.; Vasconcelos, T. R. A. Simple reduction of ethyl, isopropyl and benzyl aromatic esters to alcohols using sodium borohydride-methanol system. *ARKIVOC* **2006**, 128-133.
18. Boechat, N.; da Costa, J. C. S. D.; Souza Mendonca, J. D. S.; Oliveira, P. S. M. D.; Souza, M. V. N. D. A simple reduction of methyl aromatic esters to alcohols using sodium borohydride-methanol system. *Tetrahedron Lett.* **2004**, *45* (31), 6021-6022.

19. Han, S. Y.; Lee, H. S.; Choi, D. H.; Hwang, J. W.; Yang, D. M.; Jun, J. G. Efficient Total Synthesis of Piceatannol via (E)-Selective Wittig-Horner Reaction. *Synth. Commun.* **2009**, *39*, 1425-1432.
20. Lee, D. H.; Kim, S. Y.; Hong, J.-I. A Fluorescent Pyrophosphate Sensor with High Selectivity over ATP in Water. *Angew. Chem. Int. Ed.* **2004**, *43* (36), 4777-4780.
21. Liu, D. J.; Credo, G. M.; Su, X.; Wu, K.; Lim, H. C.; Elibol, O. H.; Bashir, R.; Varma, M. Surface immobilizable chelator for label-free electrical detection of pyrophosphate. *Chem. Commun.* **2011**, *47* (29), 8310-8312.
22. Knölker, H. J.; Fröhner, W.; Heinrich, R. Transition Metal Complexes in Organic Synthesis, Part 74: [1] Total Synthesis of the Marine Alkaloid 6-Chlorohyellazole. *Synlett* **2004**, *15*, 2705-2708.
23. Yoo, W. J.; Yuan, H.; Miyamura, H.; Kobayashi, S. Facile Preparation of 2-Substituted Benzoxazoles and Benzothiazoles via Aerobic Oxidation of Phenolic and Thiophenolic Imines Catalyzed by Polymer-Incarcerated Platinum Nanoclusters. *Adv. Synth. Catal.* **2011**, *353* (17), 3085-3089.
24. Wu, I. T.; Chaing, P. Y.; Chang, W. J.; Sheu, H. S.; Lee, G. H.; Lai, C. K. Columnar/smectic metallomesogens derived from heterocyclic benzoxazoles. *Tetrahedron* **2011**, *67* (38), 7358-7369.
25. Chang, J.; Zhao, K.; Pan, S. Synthesis of 2-arylbenzoxazoles via DDQ promoted oxidative cyclization of phenolic Schiff bases—a solution-phase strategy for library synthesis. *Tetrahedron Lett.* **2002**, *43*, 951-954.
26. Varma, R. S.; Kumar, D. Manganese triacetate oxidation of phenolic schiffs bases: Synthesis of 2-arylbenzoxazoles. *J. Heterocyclic Chem.* **1998**, *35* (6), 1539-1540.
27. Pawar, S. S.; Dekhane, D. V.; Shingare, M. S.; Thore, S. N. Alum ($KAl(SO_4)_2 \cdot 12H_2O$)-Catalyzed, Eco-Friendly, and Efficient One-Pot Synthesis of 2-Arylbenzothiazoles and 2-Arylbenzoxazole in Aqueous Medium. *Aust. J. Chem.* **2008**, *61* (11), 905-909.
28. Stephens, F. F.; Bower, J. D. The preparation of benziminazoles and benzoxazoles from Schiff's bases. Part I. *J. Chem. Soc.* **1949**, 2971-2972.
29. Srivastava, R. G.; Venkataramani, P. S. Barium Manganate Oxidation in Organic Synthesis: Part III: Oxidation of Schiff's Bases to Benzimidazoles Benzoxazoles and Benzthiazoles. *Synth. Commun.* **1988**, *18* (13), 1537-1544.
30. Praveen, C.; Kumar, K. H.; Muralidharan, D.; Perumal, P. T. Oxidative cyclization of thiophenolic and phenolic Schiff's bases promoted by PCC: a new oxidant for 2-substituted benzothiazoles and benzoxazoles. *Tetrahedron* **2008**, *64* (10), 2369-2374.
31. Tagawa, Y.; Koba, H.; Tomoike, K.; Sumoto, K. Synthesis of Caboxamycin and Its Derivatives Using Eco-Friendly Oxidation. *Heterocycles* **2011**, *83* (4), 867-874.
32. Henderson, S. J.; Xia, J.; Wu, H.; Stafford, A. R.; Leslie, B. A.; Fredenburgh, J. C.; Weitz, D. A.; Weitz, J. I. Zinc promotes clot stability by accelerating clot formation and modifying fibrin structure. *thrombosis and haemostasis* **2016**, *115* (3), 533-42.

33. Hackley, B. M.; Smith, J. C.; Halsted, J. A. A Simplified Method for Plasma Zinc Determination by Atomic Absorption Spectrophotometry. *Clin. Chem.* **1968**, *14*, 1.
34. Marx, G.; Korner, G.; Mou, X.; Gorodetsky, R. Packaging zinc, fibrinogen, and factor XIII in platelet α -granules. *J. Cell. Physiol.* **1993**, *156* (3), 437-442.
35. Tubek, S.; Grzanka, P.; Tubek, I. Role of Zinc in Hemostasis: A Review. *Biol. Trace Elem. Res.* **2008**, *121*, 1-8.
36. Mahdi, F.; Madar, Z. S.; Figueroa, C. D.; Schmaier, A. H. Factor XII interacts with the multiprotein assembly of urokinase plasminogen activator receptor, gC1qR, and cytokeratin 1 on endothelial cell membranes. *Blood* **2002**, *99* (10), 3585-3596.
37. Vu, T. T.; Fredenburgh, J. C.; Weitz, J. I. Zinc: An important cofactor in haemostasis and thrombosis. *Thromb Haemost* **2013**, *109* (03), 421-430.
38. Uppal, R.; Ciesienki, K. L.; Chonde, D. B.; Loving, G. S.; Caravan, P. Discrete Bimodal Probes for Thrombus Imaging. *J. Am. Chem. Soc.* **2012**, *134*, 10799-10802.

Graphics Abstract



An efficient synthesis route is found to give Zinhbo compounds that give NIR-emission upon binding Zn^{2+} in cellular environments.

Highlights

- Efficient synthesis for construction of a zinc probe
- Zinc binding to induce NIR emission from excited state intramolecular proton transfer
- NIR-emission with large Stokes shift
- Zinc binding response for thrombus imaging

Declaration of interests

☒ The authors declare that they have no known competing financial interests or personal relationships that could have appeared to influence the work reported in this paper.

☐ The authors declare the following financial interests/personal relationships which may be considered as potential competing interests: